ChemComm

COMMUNICATION

View Article Online
View Journal | View Issue

Cite this: *Chem. Commun.*, 2015, **51**, 13213

Received 25th May 2015,
Accepted 9th July 2015

DOI: 10.1039/c5cc04281j

www.rsc.org/chemcomm

Insight into the esterase like activity demonstrated by an imidazole appended self-assembling hydrogelator†

Nishant Singh,[a] Maria P. Conte,[b] R. V. Ulijn,*[bc] Juan F. Miravet*[a] and Beatriu Escuder*[a]

A low molecular weight hydrogelator with a covalently appended imidazole moiety is reported. Capable of percolating water in the pH range of 6 to 8, it proves to be an efficient catalyst upon self-assembly, showing Michaelis–Menten type kinetics. Activities at different pH values correlated with dramatic structural changes were observed. It can hydrolyse *p*-nitrophenyl acetate (*p*NPA) as well as inactivated esters, and L and D-phenylalanine methyl esters. The enhanced activity can be related to the conglomeration of catalytic groups upon aggregation resulting in their close proximity and the formation of hydrophobic pockets.

Mimicking and emulating enzymes by means of synthetic catalysts is currently an area of huge interest.[1] Tertiary structures allow various functional groups to be precisely arranged in three-dimensional space, creating sites to bind substrates and positioning chemical functional groups to enable catalysis. The prediction and synthesis of enzyme performance from *de novo* designed primary sequences able to fold and function accordingly is currently not possible. However, it is possible to attain enzyme-like activity by using smaller self-assembling molecules or peptides owing to the ordered arrangement of the catalytically active sites/functional groups. Several groups have demonstrated esterase-like activity using metal based nanoparticles, micelles or dendrimers with large molecular weights and mostly with spherical symmetry.[2] Histidine-containing peptide nanofibrillar systems have been reported recently as catalysts for activated ester hydrolysis (2,4-dinitrophenyl acetate and *p*-nitrophenyl acetate) and have revealed the role of the fibrillar nanostructure and multivalency in the catalytic performance.[3] In this communication we report a low molecular weight hydrogelator (**1**) with covalently linked imidazole moieties demonstrating esterase like activity. The ordered arrangement of the catalytic centres upon self-assembly of molecules into a fibrillar network is taken advantage of to attain improved catalytic activity when compared to the non-aggregating analogue. In contrast to previously reported examples, **1** is a small synthetically simple compound that is able to hydrolyse not only activated but also non-activated aminoacyl esters (Scheme 1).[3]

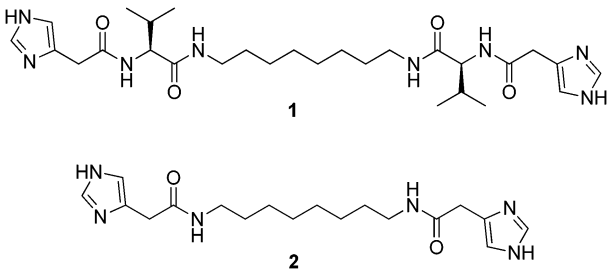

Scheme 1 Self-aggregating compound **1** and non-aggregating analogue **2**.

Compound **1** with a minimum gel concentration of 5.7 mM was tested for the esterase like activity using *p*NPA as the substrate. *p*NPA upon hydrolysis yields chromogenic *p*-nitrophenolate anion which can be monitored at 400 nm using UV spectroscopy (see ESI† for details). The initial parts of the kinetic curves for hydrolysis at different concentrations of substrate were fitted to the Michaelis–Menten equation for respective pH values. The obtained K_M, k_{cat} and V_{max} values are presented in Table 1.

The calculated pK_a values for the aggregated compound **1** are 5.9 and 6.6, with the monoprotonated species abundant in this range (see Fig. S1, ESI†). This drop in the pK_a value to 5.9 is only observed for the aggregated form of **1**, as in solution the pK_a values are similar (6.2 and 6.3). This indicates the increase in basicity of one of the two imidazole moieties in molecule **1** only in the self-assembled state.

The catalytic efficiency (k_{cat}/K_M) for imidazole molecules in solution is known to drop significantly at lower pH values.[2a,3,4]

[a] *Departament de Química Inorgànica i Orgànica, Universitat Jaume I, 12071 Castelló, Spain. E-mail: miravet@uji.es, escuder@uji.es; Fax: +34 964728214; Tel: +34 964729155*

[b] *WestCHEM/Department of Pure & Applied Chemistry, University of Strathclyde, 295 Cathedral Street, Glasgow, G1 1XL, UK*

[c] *Advanced Science Research Center (ASRC) and Hunter College, City University of New York, 85 St Nicholas Terrace, New York NY10027, USA*

† Electronic supplementary information (ESI) available: Experimental details on synthesis and characterisation of compounds and catalytic experiments. See DOI: 10.1039/c5cc04281j

Table 1 Obtained K_M, k_{cat} and V_{max} values of hydrolysis of *p*NPA by **1**

	pH 6	pH 6.5	pH 7	pH 7.5	pH 8
k_{cat} (s^{-1}) $\times 10^2$	2.6 ± 0.4	2.5 ± 0.6	2.1 ± 0.4	2.4 ± 0.7	2.5 ± 0.6
K_M (mM)	3.3 ± 1.1	3.1 ± 1.6	4.0 ± 1.5	3.9 ± 1.6	3.7 ± 1.3
V_{max} (μmol s^{-1})	8.8	8.6	7.3	8.1	8.3

The higher amounts of protonated imidazole moieties are held responsible for this which normally are not catalytically active. To our surprise, for the pH 6 and 6.5 we did not observe this drop; in fact there was a slight rise in the catalytic efficiency when compared to higher pH values like 7 and 7.5. This unusual catalytic efficiency around the pK_a values of self-assembled **1** suggests the involvement of both protonated and deprotonated imidazoles in the catalysis, often referred to as a cooperative mechanism in the literature (Fig. S2c and d, ESI†).[2a,3,4]

Well above the pK_a only the deprotonated imidazole residues are present and held responsible for the hydrolysis. The catalytic efficiency at pH 8 only due to the deprotonated imidazole groups is 7.37 M^{-1} s^{-1}. We know from the potentiometric titration curve that the mono-protonated imidazole is present in four-fold excess compared to the deprotonated imidazole at pH 6.5 (Fig. S1, ESI†). According to these values, the extrapolated catalytic efficiency of the deprotonated imidazole at pH 6.5, assuming that the protonated imidazole is not active should be 1.65 M^{-1} s^{-1} whereas that observed is 8.09 M^{-1} s^{-1}. Hence, based on these observations the catalytic efficiency at lower pH values 6 and 6.5 cannot be simply attributed to the contribution of the fraction of deprotonated imidazole. Instead, the cooperativity between both protonated and deprotonated imidazole groups is likely responsible.

The solubility (K_{sol}) of compound **1** obtained by NMR experiments for pH 6, pH 7 and pH 8 were 2.85 mM, 1.95 mM and 0.95 mM respectively (Fig. S4, ESI†). The K_{sec} (second order rate constant) values observed at these pH respective non-aggregating concentrations of compound **1**, were significantly lower than at the self-assembling concentration (Fig. S3, ESI†), thus highlighting the fact that observed catalysis is not by the molecules in solution but due to the catalytically active fibers. This was further confirmed by the catalytic activity observed for the non-assembling analogue **2**. The K_{sec} for **2** at pH 6.5, pH 7 and pH 8 are 0.5 M^{-1} s^{-1}, 0.7 M^{-1} s^{-1} and 2.2 M^{-1} s^{-1} which are significantly lower than for **1** under identical conditions. The obtained linear relationship between velocity of product formation and substrate concentration reflected the lack of any binding events unlike **1** (Fig. 1a and Fig. S2b, ESI†).

Owing to the fast hydrolysis trend shown by **1** we anticipated it to be capable of hydrolysing even stronger non-activated ester linkages such as methyl esters. We chose L and D-phenylalanine methyl esters as our substrate and followed its hydrolysis by HPLC (see ESI† for details). As expected, these substrates did not undergo any noticeable background hydrolysis at pH 7 whereas, with 33 mol% of **1** as the catalyst, we could observe a commendable hydrolysis rate of the methyl esters (Fig. 4a and Fig. S8, ESI†). The calculated catalytic efficiency for the hydrolysis of L and D-phenylalanine methyl esters by **1** are 1.2 $\times$ 10^{-3} M^{-1} h^{-1} and 1.7 $\times$ 10^{-3} M^{-1} h^{-1} respectively. The K_{sec} (2.5 $\times$ 10^{-4} M^{-1} h^{-1}) for **2** is an order of magnitude smaller than for **1** exemplifying the aggregation effect, even though there does not seem to be any stereoselectivity shown by **1** (Fig. 4b). Thus, the hydrolysis of a non-activated ester at the physiological pH, which to our knowledge has not been demonstrated before, reflects the fact that aggregation can lead to newly emergent catalytic abilities even in small molecules owing to the high local concentration of the catalytic sites.

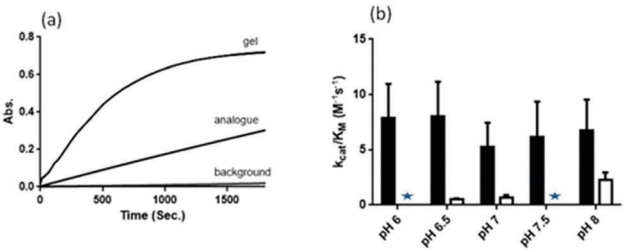

Fig. 1 (a) UV kinetic profile of *p*NPA (1.4 mM) hydrolysis at 400 nm catalysed by 0.17 Mm of compound **1** gel, compound **2** and background hydrolysis at pH 6.5. (b) k_{cat}/K_M values obtained by compound **1** at different pH values (black bars) and K_{sec} values for **2** (white bars, * not determined).

A series of experiments were performed to obtain the structure–activity relationship. The nanoscale structures of the self-assembled networks of gels as observed by TEM differ depending on pH values (Fig. 2). TEM images reveal helical fibres of 15–20 nm width at pH 6 and 6.5. The higher V_{max} values for *p*NPA hydrolysis obtained at these pH values can be attributed to the observed high aspect ratio fibres, allowing a higher extent of substrate binding thus releasing more products. At pH 7 and 8 the molecules aggregate in flat belt-like structures, which are 0.5 μm wide and several micrometers long, with a lower aspect ratio. The variation in morphologies based on pH can be attributed to the change in the number of protonated imidazole residues. The repulsion between a higher number of protonated imidazole present at pH 6 and 6.5 may result in stacking of molecules with a higher slip angle between them; this gives rise to the twists observed in the nanofibers. This is not seen farther away from the pK_a by increasing the pH

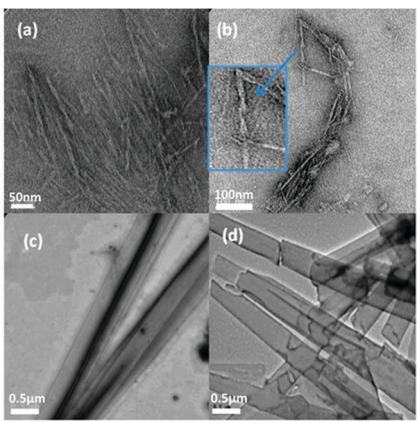

Fig. 2 TEM images of gels at (a) pH 6 (scale bar: 50 nm) (b) pH 6.5 (scale bar: 100 nm) (inset: zoomed image of twisted fibre) (c) pH 7 (scale bar: 0.5 μm) (d) pH 8 (scale bar: 0.5 μm).

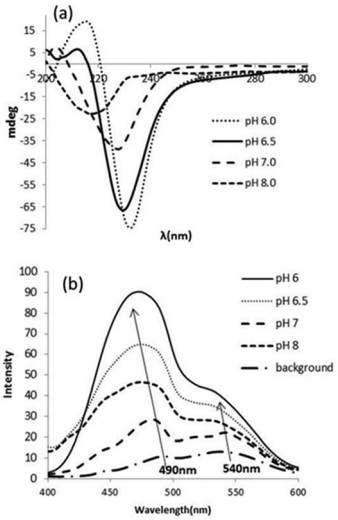

Fig. 3 (a) CD spectra obtained for gels at different pH values and (b) fluorescence emission of ANS in gels and background at different pH values.

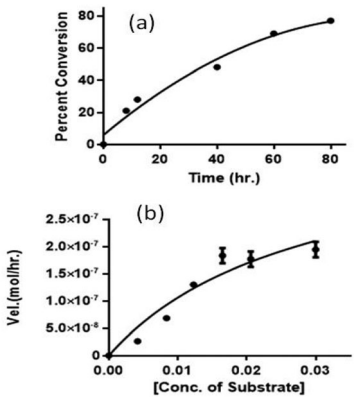

Fig. 4 (a) Product formation upon hydrolysis of L-phenylalanine methyl ester (12.3 mM) by **1** (5.6 mM) in the span of 80 hours as observed by HPLC. (b) Michaelis–Menten fitting at different concentrations for pH 7.

due to the significantly lower number of protonated imidazole residues.

The amide I′ band in the 1630–1638 cm^{-1} region of IR for different pH values denote the presence of β-sheet like structures, which is also evident from the circular dichroism (CD) contours (Fig. 3(a) and Fig. S9, ESI†). While moving from pH 8 to pH 6 an increase in ellipticity together with an apparent red-shift is observed in the CD spectra.[5a,b,d]

These kinds of spectral shifts to longer wavelengths are reported for twisted fibers having π–π* transitions with larger dipole moments which is expected in the case of protonated imidazoles more than the deprotonated ones.[5c] This information obtained from CD and IR are in agreement with the TEM images of the catalytic gels, which switch from twisted helical fibers (pH 6 and 6.5) to flat belt like structures (pH 7 and 8).

In order to evaluate the presence of hydrophobic binding pockets, we probed the gels at different pH values with 1-anilinonaphthalene-8-sulphonate (ANS), used extensively for this purpose in protein structure studies.[6] When ANS was introduced into hydrogel **1**, an apparent blue shift along with the increase in the fluorescence was observed, confirming the presence of hydrophobic pockets (Fig. 3(b)). These hydrophobic binding pockets could be formed by the central alkyl chain as well as by the L-valine isopropyl residues in **1**. The molecular rigidity introduced by the two amide groups could be balanced by the flexibility of the alkyl spacer as well as the rotational freedom of the imidazole end fragments. Overall, a dynamic binding pocket could be confirmed in the vicinity of the catalytic fragment. It is also remarkable that the effect of the L-valine residue as compound **2** lacking this amino acid fragment does not even aggregate under similar conditions. Moreover, the fluorescence intensity at pH 6 and 6.5 is higher and more blue shifted (472 nm for pH 6 and 474 nm for pH 6.5) than for the rest of the pH values, suggesting stronger binding of the ANS and supporting the lower K_M values obtained for the *p*NPA hydrolysis at these pH values. In summary, the k_{cat} observed for *p*NPA hydrolysis shows little variation with pH, with the change in catalytic efficiency probably due to differences in substrate binding. Although the errors in K_M are significant, a clear trend is observed. This behaviour can be attributed to the difference in availability of binding pockets for each morphology. It is remarkable that a simple low molecular weight self-assembling compound bearing a minimal peptidic fragment is able to catalyse the hydrolysis of an activated ester as efficiently or even better than the few previously reported examples of longer self-assembled peptides.[3] For instance, Stupp *et al.*[3a] reported a rate constant of 1.67×10^{-2} s^{-1} and a K_M of 0.4 mM for a bis-histidine containing decapeptide and a less efficient tetradecapeptide containing one histidine residue was described by Liang *et al.*[3c] (k_{cat} 0.19 × 10^{-2} s^{-1} and K_M 21.68 mM). The same group reported a shorter analogue (Fmoc–FFH–$CONH_2$) with lower reaction rate than in the case of compound **1** (k_{cat} 0.14 × 10^{-2} s^{-1}) but with a stronger binding ability (K_M 0.76 mM).[3b] Related results have been also reported by Korendovych *et al.* for amyloidogenic heptapeptides bearing H residues that after self-assembly are able to coordinate Zn^{+2} and efficiently catalyse the hydrolysis of *p*NPA.[3d] This example, however, follows a different catalytic mechanism based on a metal ion Lewis acid catalysis. All these examples highlight the existence of an undoubtable link between self-assembly and emergence of catalysis which is also exemplified by compound **1**.

In summary, we have reported an example of a catalytic supramolecular hydrogel in which binding and catalysis take place in reaction sites self-constructed solely by non-covalent interactions. We have been able to identify the probable structure–activity relationship between the different self-assembled structures and the subsequent catalytic performances of the gels. The results indicated that the presence of hydrophobic pockets, higher aspect ratio of fibres and the balance between the protonated and deprotonated imidazole could be the key factors for improved hydrolysis efficiency compared to related non-aggregating catalysts. It is remarkable that enzyme-like catalytic behaviour emerges after self-assembly of small and simple molecular components. It is worth mentioning that very simple low-molecular weight

compounds can approach, although modestly by now, what evolution has achieved after millions of years. In fact, it has been proposed that short self-assembled peptides could have played a relevant role in the early stages of the origin of life.[7] In this context, self-assembled catalytic peptides could have been potential precursors of enzymes.

This work was supported by the EU Marie Curie ITN-Smartnet and the Ministry of Economy and Competitiveness of Spain (Grant CTQ2012-37735). N.S. and M.P.C. thank EU for an ESR Marie Curie contract.

Notes and references

1 (*a*) M. Raynal, P. Ballester, A. Vidal-Ferran and P. W. N. M. van Leeuwen, *Chem. Soc. Rev.*, 2014, **43**, 1660–1733; (*b*) M. Raynal, P. Ballester, A. Vidal-Ferran and P. W. N. M. van Leeuwen, *Chem. Soc. Rev.*, 2014, **43**, 1734–1787.

2 (*a*) D. Zaramella, P. Scrimin and L. J. Prins, *J. Am. Chem. Soc.*, 2012, **134**, 8396–8399; (*b*) G. Pieters and L. J. Prins, *New J. Chem.*, 2012, **36**, 1931–1939; (*c*) G. Chadha and Y. Zhao, *Org. Biomol. Chem.*, 2013, **11**, 6849–6855; (*d*) G. Chadha and Y. Zhao, *Chem. Commun.*, 2014, **50**, 2718–2720.

3 (*a*) M. O. Guler and S. I. Stupp, *J. Am. Chem. Soc.*, 2007, **129**, 12082–12083; (*b*) Z. P. Huang, S. W. Guan, Y. G. Wang, G. N. Shi, L. N. Cao, Y. Z. Gao, Z. Y. Dong, J. Y. Xu, Q. Luo and J. Q. Liu, *J. Mater. Chem. B*, 2013, **1**, 2297–2304; (*c*) C. Zhang, X. Xue, Q. Luo, Y. Li, K. Yang, X. Zhuang, Y. Jiang, J. Zhang, J. Liu, G. Zou and X.-J. Liang, *ACS Nano*, 2014, **8**, 11715–11723; (*d*) C. M. Rufo, Y. S. Moroz, O. V. Moroz, J. Stohr, T. A. Smith, X. Z. Hu, W. F. DeGrado and I. V. Korendovych, *Nat. Chem.*, 2014, **6**, 303–309.

4 (*a*) K. S. Broo, H. Nilsson, J. Nilsson, A. Flodberg and L. Baltzer, *J. Am. Chem. Soc.*, 1998, **120**, 4063–4068; (*b*) C. Guarise, F. Manea, G. Zuapa, L. Pasquato, L. J. Prins and P. Scrimin, *J. Pept. Sci.*, 2008, **121**, 174–184.

5 (*a*) B. A. Wallace, J. G. Lees, A. J. W. Orry, A. Lobley and R. W. Janes, *Protein Sci.*, 2003, **12**, 875–884; (*b*) E. T. Pashuck, H. Cui and S. I. Stupp, *J. Am. Chem. Soc.*, 2010, **132**, 6041–6046; (*c*) U. Anand and M. Mukherjee, *Langmuir*, 2013, **29**, 2713–2721; (*d*) S. M. Kelly and N. C. Price, *Curr. Protein Pept. Sci.*, 2000, **1**, 349–384.

6 (*a*) E. Schönbrumm, S. Eschenburg, K. Luger, W. Kabsch and N. Amrhein, *Proc. Natl. Acad. Sci. U. S. A.*, 2000, **97**, 6345–6349; (*b*) G. Chadha and Y. Zhao, *J. Colloid Interface Sci.*, 2013, **390**, 151–157.

7 O. Carny and E. Gazit, *FASEB J.*, 2005, **19**, 1051–1055.

